ELSEVIER
Journal of Alloys and Compounds 293–295 (1999) 621–625
Journal of ALLOYS AND COMPOUNDS

Electrochemical characteristics of AB_5-type hydrogen storage alloys solidified at different cooling rates

L.Y. Zhang

Technology Laboratory, Energizer Power Systems, PO Box 147114, Gainesville, FL 32614-7114, USA

Abstract

Three alloys with the same formula $Mm(NiCoMnAl)_5$ were produced by vacuum induction melting and casting in different cooling rates: normal cooling, fast cooling, rapid quench. A part of the rapidly quenched alloy was annealed. Ingots of the four alloys were mechanically pulverized to <75 μm powder, and pellet electrodes were made. Half cell test results show that all the alloys have similar discharge capacity at a rate of 100 mA/g. However, at a rate of 1500 mA/g their discharge capacity strongly depends on the metallurgical processes. In order to understand the high rate capacity of these alloys, a systematic investigation was conducted. The alloy pulverization rate, alloy surface reactivity and alloy hydrogen diffusion coefficients were examined. The results are reported and discussed.

Keywords: Hydrogen storage alloy; MH Electrode; Nickel–metal hydride batteries

1. Introduction

Over the past decade, considerable research activities have been directed to improve AB_5 type hydrogen storage alloys for developing high performance NiMH batteries. Among these efforts, increasing cooling rate during solidification and heat treatment have been a topic attracting vigorous research activities. It has been found that the alloy composition, casting conditions and post heat treatment have significant influence on the capacity and cycle life of MH electrodes [1,2]. As viewed from practical applications, rate capability of MH electrode is an important property. MH electrode with higher high-rate discharge capacity can make NiMH cells deliver power at high current rate, or under normal operating be of benefit in voltage performance. In this study, the effect of metallurgical conditions on MH electrode's rate capability was investigated. Alloy pulverization rate, alloy surface reactivity and hydrogen diffusion coefficients were examined. Results of this investigation are reported and discussed in this presentation.

2. Experimental

Three alloys used in this study have the same nominal composition $MmNi_{3.6}Co_{0.7}Mn_{0.3}Al_{0.4}$ where the Mm is a La-rich mischmetal with approximate 50% La. Alloys were produced in industrial production quantity with different cooling rate during casting: normal cooling (NC), fast cooling (FC), and rapid quenching (RQ). A part of the RQ alloy was then annealed (RQ/HT). Metallurgical conditions are described elsewhere [3] and summarized in Table 1.

The ingots were mechanically pulverized to <75μm powder. Metal hydride electrodes were made by mixing 250 mg of MH powder with 250 mg of nickel powder, then cold pressed to form a pellet with a diameter of 8 mm and a thickness of about 1.5 mm. A half-cell was constructed using the MH pellet as the working electrode, a sintered $Ni(OH)_2$/NiOOH as counter electrode, a Hg/HgO reference electrode, in 30 wt.% KOH electrolyte solution. To evaluate high rate dischargeability and surface reactivity, the electrodes were cycled 15 times. In each cycle, the electrodes were charged for 4 h and discharged to 0.7 V (Hg/HgO) at a rate of 100 mA/g.

The electrochemical kinetics for the hydrogen absorp-

Table 1
Metallurgical processes of the AB_5 alloys

Alloy	Ingot thickness (mm)	Cool rate	Heat treatment
		(in order; °C/S)	
NC	30	10^1	No
FC	10	10^2	No
RQ	1	10^3	No
RQ&H/T	1	10^3	Yes

0925-8388/99/$ – see front matter
PII: S0925-8388(99)00354-0

tion and desorption process were determined by d.c. polarization methods [2]. After 15 cycle activation, the electrode was scanned at 0.1 mV/S from −20 mV to +20 mV with respect to the equilibrium potential in 25% state of charge (SOC). The linear polarization enables us to calculate the surface charge transfer reaction kinetic parameters (i.e., the exchange current; *J* in mA/g).

The hydrogen diffusion coefficients in the bulk alloys can be measured using electrochemical technique [4,5]. In this study, the potential step technique was employed. The activated electrodes were charged and then discharged to ~5% of its full capacity. After the electrode's equilibrium potential was established, a potentiostatic pulse of +200 mV/g vs. OCV was applied, and a chronoamperometric curve was obtained, which corresponds to the diffusion-limited regime. Assuming semi-infinite linear diffusion conditions, the current may be expressed as [6,7]

$$i = -FD_{\mathrm{H}}C^{\mathrm{o}}[1/(t\pi \mathrm{D}_{\mathrm{H}})^{1/2} - 1/\mathrm{r}_{\mathrm{o}}]$$

where *i*: current at time *t*; *F*: Faraday constant; C^{o}: hydrogen density in alloy before test; r_{o}: radius of MH particle; *S*, *I*: slope and intersection of *J* vs. $t^{-0.5}$ plot, respectively. Therefore, the diffusion coefficient can be obtained from the *S, I,* and particle radius from

$$D_{\mathrm{H}} = [r_{\mathrm{o}}\pi^{1/2} \times I/S]$$

3. Results and discussion

All the experiments were conducted at room temperature (21°C). The data obtained are summarized in Table 3.

3.1. Rate capability

After 15 cycle activation, the electrodes were fully charged and then discharged in two steps: firstly the electrode was discharged at 1500 mA/g (5 C_{A}) and cut off at 0.5 V with respect to Hg/HgO, followed by a secondary discharge at 60 mA/g ($C_{\mathrm{A}}/5$) to 0.7 V. A theoretical alloy capacity of 300 mAh/g, designated as C_{A}, was taken for all the alloys. The capacities obtained from the two step discharge were added up as capacity at $C_{\mathrm{A}}/5$ rate. The percentage of 5 C_{A} discharge capacity with respect to the $C_{\mathrm{A}}/5$ discharge capacity was used to describe the alloy's high rate discharge efficiency (HRDE), as illustrated in Fig. 1. The high rate dischargeability depends on metallurgical conditions and is in the following order:

$$\mathrm{NC} > \mathrm{FC} > \mathrm{RQ} > \mathrm{RQ/HT}$$

While the three as-cast alloys perform similarly, the RQ/HT alloy displays substantially lower HRDE.

3.2. Pulverization rate

Alloy pulverization behavior was investigated. Alloy powder materials used in the electrodes were pulverized using gas phase hydriding and dehydriding method (H/D). The particle size (PS) and specific surface area (SA) were analyzed using MicroTrac and BET technique, respectively. The PS is represented in terms of *d*(50) which is a characteristic diameter. For example, a *d*(50) value of 35 μm means that 50% of the sample volume is occupied by particles having diameter of not more than 35 μm. The percentage of PS breakdown and SA enlargement of alloy powders with H/D cycles is plotted in Figs. 2 and 3. After 15 H/D cycles, the percentage of PS breakdown and the

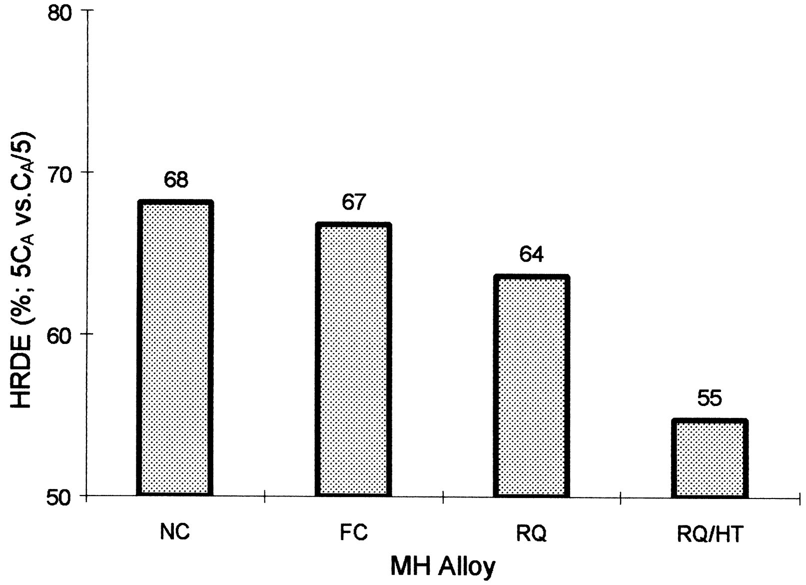

Fig. 1. Influence of metallurgic conditions on the high rate discharge efficiency (HRDE) of MH electrodes.

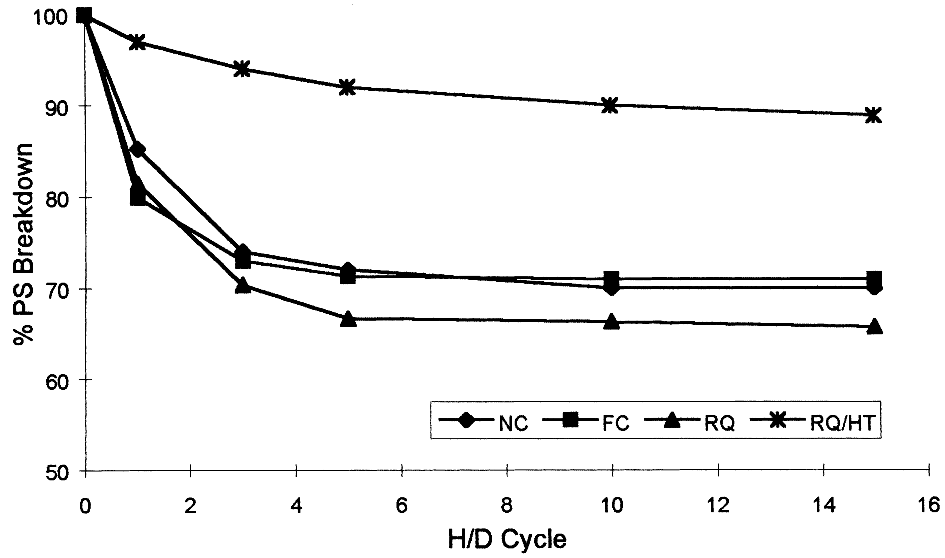

Fig. 2. Change in MH alloy particle size (PS) as a function of gas phase H/D cycling. The original PS of each alloy powder was taken as 100%.

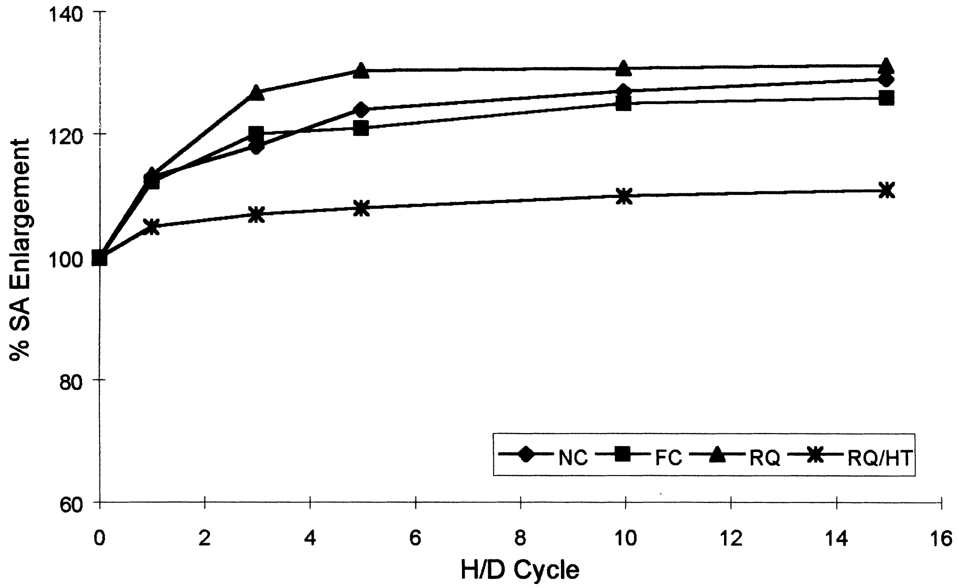

Fig. 3. Change in MH alloy specific area (SA) as a function of gas phase H/D cycling. The original SA of each alloy powder was taken as 100%.

percentage of SA enlargement are listed in Table 2, displaying pulverization rate. Apparently, all the as-cast alloys have similar pulverization rate, while the RQ/HT alloy exhibits the least. This observation suggests that the elemental segregation, lattice defects and mechanical stress generated during casting are the major causes of fast pulverization of as-cast alloys.

Table 2
Pulverization rate of MH alloy particles

Alloy	NC	FC	RQ	RQ/HT
% of PS	70	71	66	89
% of SA	129	126	131	111

3.3. Surface reactivity

According to results of linear polarization analysis, the alloy surface reactivity of each alloy (the exchange current J; mA/g) was calculated. Assuming that the break down of MH particles during electrochemical cycling occurs in the same way as during gas phase H/D cycling, the alloy

Table 3
Characteristics of MH electrodes (21°C)

Alloy	Capacity (mAh/g)		At 15th cycle		Exch. Current	Exch. Curr. Density (J_o; mA/cm^2)	H Diff. Coeff. (D_H; cm^2/S)
	(at 60 mA/g)	(at 1500 mA/g)	(PS; μm)	(SA; m^2/g)			
NC	296	201	26	0.318	112	0.0352	3.23×10^{-8}
FC	293	196	24	0.323	122	0.0378	4.35×10^{-8}
RQ	288	187	26	0.297	116	0.0395	2.45×10^{-9}
RQ/HT	301	166	33	0.251	96	0.0382	5.02×10^{-8}

surface catalytic reactivity (exchange current density J_o; mA/cm^2) was estimated according to

$$J_o = J/\mathrm{SA}$$

The results are listed in Table 3. It can be seen that all the MH alloys exhibit similar exchange current density (~0.04 mA/cm^2). However, the RQ/HT alloy has the lowest SA, as well as the lowest exchange current, which is reflected by the lowest discharge capacity at 5 C_A rate.

3.4. Hydrogen diffusion coefficient

Hydrogen diffusion coefficients (D_H) in bulk MH alloys were obtained by potential step analysis. The data are summarized in Table 3, and also illustrated in Fig. 4. As shown, the D_H of as-cast alloys are strongly dependent on cooling rate, and the RQ alloy has the lowest D_H value. The difference of D_H values between the RQ and RQ/HT indicates that the heat treatment significantly improves the hydrogen diffusion rate in the bulk MH alloy. It is easily understood that the lattice defects such as dislocations, lattice vacancies, microvoids, strain field and grain boundaries are generated during casting and strongly depend on cooling conditions. These defects may trap hydrogen and hence hinder hydrogen diffusion. It is evident that some of the defects can be reduced or eliminated by annealing, since the diffusion of hydrogen in the RQ alloy was enhanced by annealing. However, high D_H of RQ/HT alloy does not display better discharge capacity at 5 C_A rate as compared to the other alloys. Since the D_H values are ~10^{-9} cm^2/s or higher, and the PS is around 30 μm, the hydrogen diffusion coefficient probably is not the limiting factor when electrodes were discharged at a rate of 1500 mA/g [8].

4. Concluding remarks

Based on the study of industrial production alloys, metallurgical conditions strongly affects MH electrode rate capability. In the discharge rate range of C_A/5 to 5 C_A, the high rate discharge efficiency (HRDE) was not improved with fast cooling rate during casting, but was hindered substantially by heat treatment.

The hydrogen diffusion coefficient of rapidly quenched alloy was dramatically decreased as compared with normally cooled and fast cooled alloys, but was significantly enhanced by annealing.

The alloy pulverization rate upon H/D cycling varies

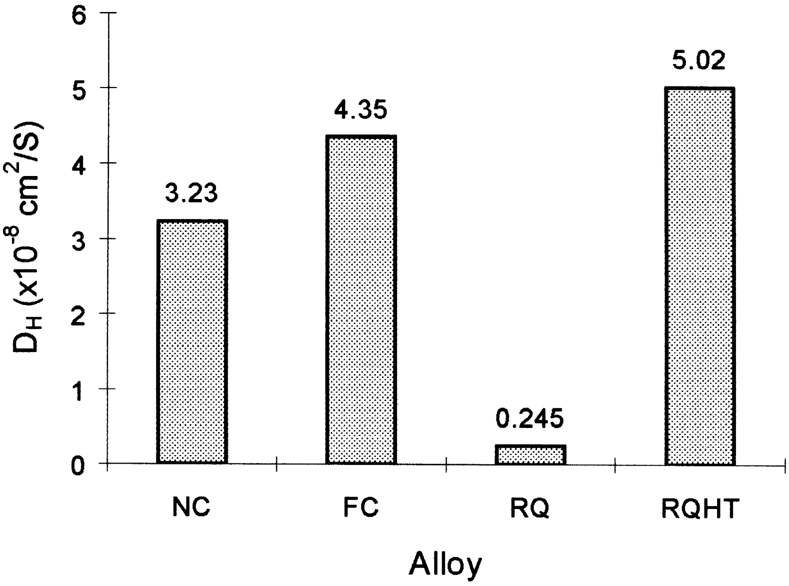

Fig. 4. Illustration of diffusion coefficients obtained form potential step analysis.

with metallurgical processes. All the as-cast alloys have similar pulverization rate, while the RQ/HT pulverizes the least.

All the alloys studied here exhibit essentially the same value of exchange current density (J_o, mA/cm^2). This result indicates that the alloy surface catalytic reactivity is determined by its chemistry, but insensitive to the metallurgical processes. The trend in HRDE of these alloys displays good agreement with alloy surface reactivity (J in mA/g) which was mainly determined by the alloy specific area (SA) within the experiment limit.

The results suggest that under the alloy production conditions in this study, for $Mm(Ni-Co-Mn-Al)_5$ electrodes discharged at a rate of 1500 mA/g at room temperature after 15 cycle activation, the hydrogen diffusion is not the limiting factor. However, the specific area, which is related to alloy pulverization rate, plays a predominant role.

References

[1] T. Sakai, H. Miyamura, N. Kuriyama, J. Alloys Comp. 191 (1993) 155–157.

[2] P.H.L. Notten, P. Hokkeling, J. Electrochem. Soc. 138 (7) (1991) 1877.

[3] L.Y. Zhang, T.J. O'Hara, M.G. Michal, presented in the International Symposium of Metal Hydrogen Systems, Hangzhou, China, October 4–9, 1998.

[4] M.H.J. van Rijawick, Hydrides for Energy Storage, in: A.F. Andersen, A.J. Maeland (Eds.), Pergamon, 1977, pp. 261–271.

[5] T. Nishina, H. Ura, I. Uchida, J. Electrochemi. Soc. 144 (4) (1997) 1273–1277.

[6] C. Cai, D.J. Zhao, B.C. Wang, Chinese Journal of Power Sources, Vol. 17 No. 5, 94 (1993) 9–13.

[7] Y. Luo, L. Kang, Y. Lei, Y. Zhou, Chinese Journal of Power Sources Vol. 21 No. 4, 117 (1997) 147–152.

[8] L.Y. Zhang, Rare Earths: Science, Technology & Applications, Renato Bautista, Charles Bounds, Timothy Ellis, Barry Kilbourn (Eds.), TMS (Minerals, Metals, Materials), 1997, pp. 235–257.